

On Verification of Splines Based Intraoperative Reconstruction of Cardiac Anatomy: Model Research

Yifan Fu, Jian Wu

Abstract—Three-dimensional (3D) endocardium visualization plays an extremely important role in localization and ablation of target areas and can improve the cure rate in computer-aided cardiac surgery. In this paper, we discuss how to reconstruct and update the corresponding endocardium surface model quickly and accurately based on the sparse point cloud that is collected dynamically on the left atrial intima. Firstly, we construct a specific mesh model, and then collect spatial points, and carried out the mesh grid approximation based on Thin Plate Splines (TPS) intra-operatively, finally, we obtained an approximate target shape after Taubin-based smooth. Experiments on four left atriums' (LA) CT Angiographies (CTA) demonstrated that the reconstructed surfaces can well fit to the target shape, the distance error of surface between the reconstructed and targets can meet clinical requirements, and the deformation time can also meet the need of real-time update. The results showed that our proposed method is robust, fast and flexible to implement.

I. INTRODUCTION

Atrial Fibrillation (AF) that is caused by abnormal electrical activity that mainly occurs in LA is a high mortality cardiovascular disease. Clinically, radio-frequency catheter ablation (RFCA) has been introduced to ablate target positions for atrial fibrillation cure.

The image navigation in AF surgery can assist surgeons to locate the location of lesions quickly, which is intuitive, accurate and can help to improve the cure rate. In current, two image processing modes are adopted: one is that using a preoperative model for deforming it to patient during surgery, which can provide detailed local surface as well as the ostiums and branches of pulmonary vein, but there still exists elastic deformation error between preoperative and intra-operative model. It is difficult to compensate by state of the art registration algorithms. Another one is the adoption of intra-operatively constructed model. Combining with position sensor, the intraoperative constructed model is accurately corresponded to the patient in operation room, the difficulty lies in the restoration of the target geometry from extremely limited information (spatial point cloud or spatial profile curve).

An algorithm is proposed and verified in this paper for the dynamic reconstruction and update of the corresponding structure from the sparse and scatter point acquired on the inner surface of LA. In image guided surgery, the navigation

image must correspond to the real target shape [1] and meet the real-time requirement, therefore there will not exist an apparent latency between data acquisition and model construction. Furthermore, the random acquisition of the procedure also imposes sparse and scatter sample point constraints on the surface reconstruction. Spatial point is dynamically collected on endocardium and the surface is updated to provide an accurate image navigation considering both overall shape and local detail in AF surgery, meanwhile LA body and the pulmonary vein ostium are identified to assist the surgeon perform circumferential pulmonary vein ablation (CPVA) and target areas ablation.

II. METHODS

A specific endocardium grid model is first built according to the initial captured points, and then deformed under the certain constraints to approximation the target shape. Figure 1 illustrates the schematic diagram of proposed method.

A. Model Construction and Alignment

The choice of a grid model is associated with the geometry of the anatomy to be reconstructed. Where G represents the grid model, $g_i = (g_{ix}, g_{iy}, g_{iz}) (i = 1, 2, \dots, N_G)$ represent the i -th vertex on G , spherical polar model is used to calculate the coordinates, the radius is constrained by the initial captured point cloud P , the number of vertex N_G is defined by a predetermined accuracy σ . Topology is established in accordance with voronoi regulation to triangulate the vertices. The resulting grid model is then calibrated to the initial point cloud by centroid matching.

B. Initial Deformation

The initial deformation for grid model is a precondition for getting an accurate and fast surface modification based on TPS, which solves the problem of global and local information lacking when the contact points is insufficient [2]. $f(g_i)$ represents the transformation of the i -th vertex g_i ($g_i \in G$) from grid model to the initial deformation.

$$f(g_i) = c_1 f(g_i)_{Chiang} + c_2 f(g_i)_{Shepard} \quad (1)$$

f_{Chiang} represents the global reverse weighted sum criteria adopted from the Chiang's method [5], where each vertex g_i on the grid model is adjusted as a weighted sum of the inverse radial distance of the grid vertex from the contact points. This procedure ensures a global shape approximation of the entire grid mesh to the initial collected contact points [4-5].

Resrach supported by the National Natural Science Foundation of China (NSFC) Grant No. (81000649), and the Knowledge Innovation Program of Basic Research Projects of Shenzhen Grant No. JCY20130402145002404.

The authors are all with the Shenzhen Key Laboratory for Minimally Invasive Medical Technologies, Graduate School at Shenzhen, Tsinghua University, Shenzhen 518055 China (tel: +86-755-26036353; e-mail: wuj@sz.tsinghua.edu.cn, fuyf11@mails.tsinghua.edu.cn).

$$f(g_i)_{Chiang} = \tilde{\lambda}_i \sum_{j=0}^{N_p} \frac{\rho_j \vec{v}_{ij}}{|\vec{v}_{ij}|^{\sigma_1} + \varepsilon} / \sum_{j=0}^{N_p} \frac{\rho_j}{|\vec{v}_{ij}|^{\sigma_1} + \varepsilon} \quad (2)$$

$$f(g_i)_{Shepard} = \tilde{\lambda}_i \sum_{g_j \in s_i} \frac{\vec{\omega}_{jj'}}{|\vec{\omega}_{jj'}|^{\sigma_2} + \zeta} \quad (3)$$

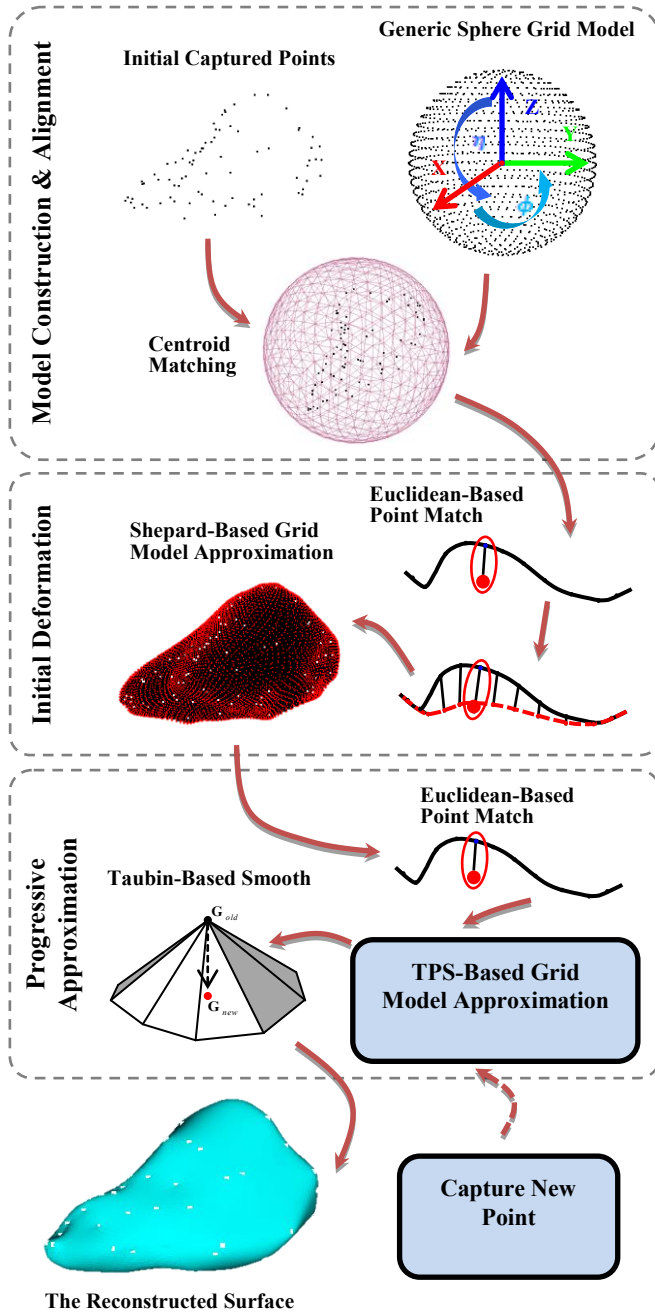


Figure 1. Schematic diagram of proposed endocardia reconstruction method.

$f_{Shepard}$ represents the neighboring weighted criteria based on the principle of Shepard, which consider a weighted sum vector for each contact point p_j ($p_j \in P$) to its matching point p'_j ($p'_j \in G'$) on grid model G within the neighboring area of each grid vertex. This item tends to attract grid vertices to move to densely sampled regions to preserve local surface details.

In (3) $\vec{\omega}_{jj'} = 1/p'_j - p_j$, p'_j is the point which make $\vec{\omega}_{jj'}$ the Euclidean distance minimal for all the points pairs in the neighborhood area s_i of the vertex g_i on grid model, ζ is a small number to prevent division by zero, c_1 and c_2 are constants to scale the weighted of f_{Chiang} and $f_{Shepard}$.

C. Progressive Approximation

The initial deformation provides an initial contribution to the following model update procedure. For each contact point the corresponding match vertex on grid model is computed using the method described in section 2.B. G'_n represents the corresponding pairs to P_{n+1} after the $n+1$ -th contact point is captured. $T_n = (f, g, h)_n : \mathbb{R}^3 \rightarrow \mathbb{R}^3$ represents the deform vectors from G_n to G_{n+1} . Solving T_n is equivalent to minimizing the cost equation of $E(T_n)$ where

$$E(T_n) = \frac{1}{N} \sum_{i=0}^{N-1} \|p_i - T_n(g'_i)\|^2 + \tau \cdot \Phi(T_n) \quad (4)$$

The TPS interpolation [6] is adopted to compute (4) after the initial deformation is completed, and a new contact point is acquired. The deformation under the constraint of TPS rules can be expressed as a series of linear equations, the computation expense is minimized and the non-convergence using optimization is avoided as well. Taubin operator [2] is used to eliminate surface wrinkle in densely sampled areas. For details of the approximation method, refer to [3].

D. Local Area Dynamic Refinement

The update time for each added contact point increases linearly with the number of point if we take successive reconstruction and update the surface mesh according to the original data. The analysis of the deform vectors showed that a new added point only affect the nearby grid vertices. Accordingly, the strategy of dynamic update is modified to deform vectors for the points in the neighboring area of each new added point. The radius is calculated by (5), and TPS interpolation is adopted as the adjustment strategy.

$$R_n = \begin{cases} +\infty & , N_{pn} < N_{def} \\ b - \kappa \cdot N_{pn} & , N_{pn} \geq N_{def} \end{cases} \quad (5)$$

Where b represents the range of area intended to select, N_{pn} represents the number of contact point, κ is a factor less than 0.5 to reduce the impact area of new added point when the number of contact point increases. When N_{pn} is less than the predefined value N_{def} , all of the deform vector for grid vertices are computed, while when N_{pn} is larger than N_{def} , the vertices needed to be adjusted on the grid is determined by R_n .

III. RESULT AND DISCUSSION

The algorithm is implemented on an Intel Pentium 3.0 GHz processor system, with Visualization ToolKit (VTK) as the visualization module. The experiment data are coronary CTA images scanned by PHILIPs Brilliance 64-slice spiral CT. 75 percent phase of heart cycle was chose to take the bilateral filtering as preprocess, region grow and Active Counter Models (ACM) are adopted to extract the anatomy of the left atrial endocardia, some undesirable images are manual corrected. Marching Cube is adopted to visualize the surface model of LA. To emulate the heart mapping procedure in AF surgery, contact points are sampled dynamically on the 3D visualization model in an irregular fashion. The point acquisition process is simulated in the laboratory according to the standard 3D modeling process in AF surgery, a group of circular points are selected at the pulmonary vein branch to isolate pulmonary and LA, the rest of contact positions are selected by the operator randomly. The acquired points are used to reconstruct and update the surface progressively by the proposed method.

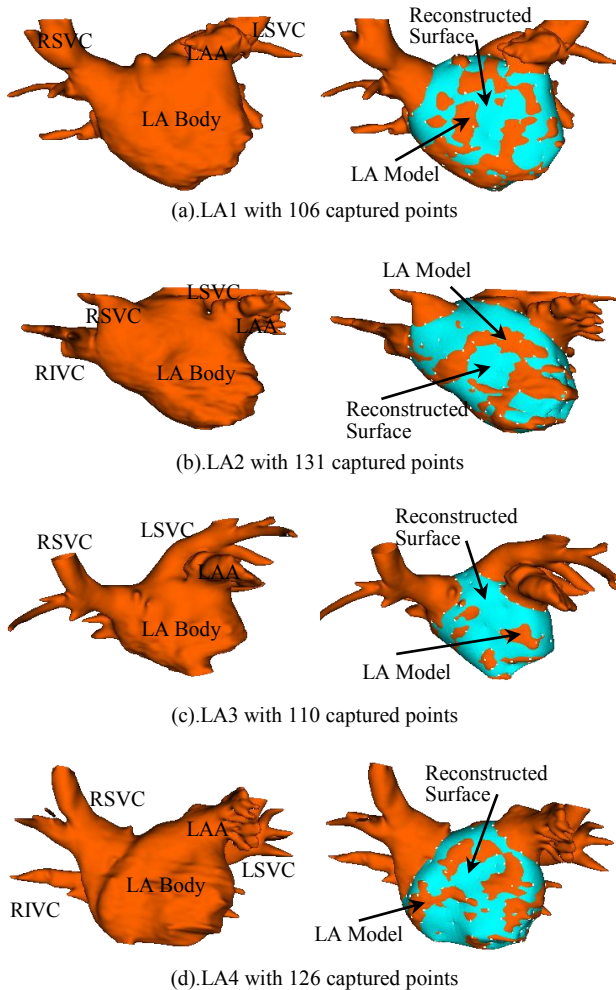


Figure 2. Superimposed comparison between CT and surface reconstructed with proposed method. (a)-(d) are 4 LA models with different captured points. The left column represented for CT LA models indicated in brown and the right column represented for the reconstructed surfaces indicated in green.

Figure 2 shows the superimposed results of the reconstructed surface and the corresponding CT surface model for four groups of different LA. The algorithm strikes a

balance in global and local detail preserving. It can be observed the TPS deformation combined with the first approximation provides a reasonable surface fitting error for the set of contact points, in spite of some sharp area like atrioventricular valve and isthmian areas that will not impact the ablation procedure. These indicate the possibility of real-time reconstruction and image guide in AF surgery.

A. Single Model Evaluation

To verify the real-time performance for single model, 106 contact points are captured dynamically on the visualization model of LA1, the process time (time represents an average of 20 sets of reconstructions) between data acquisition and model update is recorded when every new contact point is added. Figure 3 provides the fit plot of refinement time for a range of 4-106 contact points.

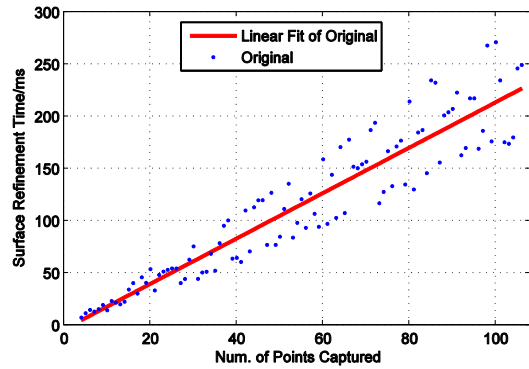


Figure 3. Dynamic refinement time fit curve of LA1.

The fit curve of Figure 3 demonstrates a linear increment between the reconstruction time and the number of contact points. The modified curve using the Local Area Dynamic Refinement method described in section 2.D is shown in Figure 4.

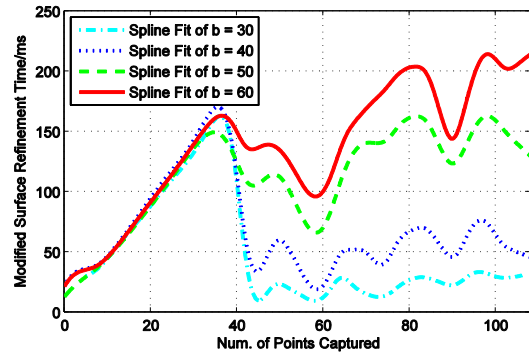


Figure 4. Modified local area dynamic refinement time fit curve of LA1

The modified time curve shows a certain level of volatility while the overall tendency is stable when the contact point increases. This type of variation is affected by the computer system and the software environment. The computation time would be a bit more than before modified if the computation cost of finding vertices that is inside of nearby area is considered, but this effect will be compensated or even ignored when the number of contact point increases. The parameter in Figure 3 is chose by experience, there need more exploration to decide this parameter in practice.

To measure the reconstruction error, 102 points are selected randomly and are taken as error evaluation points. A distance error-fit metric is defined as the normal distance per evaluation point from the corresponding nearest vertex on grid model. The distance error fit plot of the maximum, average and median error for a range of 4-106 contact points are shown in Figure 5.

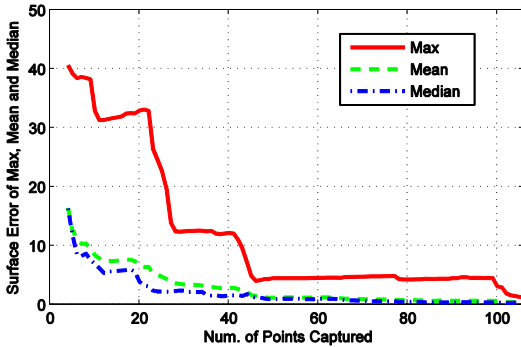


Figure 5. Error distribution curve of LA1 (with 102 evaluation points)

The contour shape and the fit error of the reconstructed surface are mainly affected by the number of contact points. The TPS deformation method has a maximum distance error above 10mm for less than 40 contact points that is the threshold to roughly determine the contour of the shape, while has a stabilized error that is about 3mm for over 41 contact points onwards which help to refine the local surface details. The above data correspond to LA1 demonstrate a 106 contact point cloud can make the reconstructed surface have the maximum error of 1.272mm, the average error of 0.434mm and the median error of 0.375mm which satisfies the accuracy requirement in image-guided surgery.

B. Statistical Analysis

To verify the consistency and effectiveness of the proposed method for different forms of LA anatomy, four groups of LA are reconstructed dynamically. Table 1 summarizes the size of LA (the maximum distance among all the points on the LA), the total number of sample points, the number of vertices on grid model, the average update time, the overall reconstruction time and the max surface error for each individual data.

TABLE I. STATISTICAL DATA FOR MULTIPLE LA RECONSTRUCTION

LA Data	Size/cm	N_p	N_G	Mean update time/ms	Overall update time/ms	Max surface error/mm
LA1	6.72	106	5402	116	525	1.272
LA2	8.06	131	6164	166	823	1.594
LA3	5.7	110	4058	116	416	1.517
LA4	6.5	126	3752	118	438	1.667

Time data represents an average of 20 sets of reconstructions

The number of vertices needed to reconstruct the grid model is proportional to the size of LA, as we mentioned in section 2.A. The grid model is specific to the anatomy to be reconstructed. The increase of contact points and grid vertices will increase the update time, as expected. Adjustment of the

strategy of refinement can make the time took per reconstruction stable in a certain extent, which has an average of 100-200ms. The overall reconstruction time after all the contact points being acquired ranges several hundred millisecond (the time is composed of initial deformation and TPS-based reconstruction), which indicates that the proposed algorithm can reconstruct the 3D model from sparse data sets without causing visual delay.

The statistical analysis of four groups of LA shows that the error of surface model is 0-1.272mm for LA1, 0-1.594mm for LA2, 0-1.517mm for LA3 and 0-1.667mm for LA4 respectively. The maximum reconstruction error of 4 LA were all less than 1.7mm, which satisfies the clinical requirements. The error mostly distributes between the range of 0.2-0.6mm, which indicates a good approximation of the reconstructed shape to the real anatomy. The maximum error are at areas with high distortion, and the complexity of the surface cannot be recovered by sparse distributed points. But the increase of sampling density can decrease the local error. The result of Table 1 demonstrates the shape of LA can be restored by a small number of points (100-200 points) with high accuracy.

IV. CONCLUSION

Experiment result show that the proposed method is capable of generating a natural and smooth shape that fits to contact point set closely that collected from the endocardium of LA dynamically, which satisfies the requirements of minimal latency and highly precision in image guided surgery. The innovation of this algorithm lies in the use of grid model and linear matrix operations to solve the iterative problem, which updates the target surface in real time. The TPS kernel combined with grid model can fit the endocardium pretty well. The reconstruction error can satisfy the clinical requirement, which demonstrates the possibility and feasibility to apply this method into real cardiac surgery.

ACKNOWLEDGMENT

Authors would like to thank Shenzhen Hospital of Traditional Chinese Medicine for their coronary CTA images.

REFERENCES

- [1] H. Liviyatan, Z. Yaniv and L. Joskowicz, "Gradient-based 2-D/3-D rigid registration of fluoroscopic X-ray to CT," IEEE Transactions on Medical Imaging, vol. 22, no. 11, pp. 1395-1406, 2003.
- [2] G. Taubin, "A signal processing approach to fair surface design," SIGGRAPH'95 Proceedings, Aug. 1995, pp. 351-358.
- [3] F. Yifan and W. Jian, "A Real-Time 3D Endocardium Surface Reconstruction Method Based on Sparse and Scatter Data," Application Research of Computers, 2014, in press.
- [4] Method and apparatus for real time quantitative three-dimensional image reconstruction of a moving organ and intra-body navigation, Official Gazette of the United States Patent and Trademark Office Patents, 2008.
- [5] P. Chiang, J. M. Zheng, K. H. Mak, N. M. Thalmann and Y. Y. Cai, "Progressive surface reconstruction for heart mapping procedure," Computer Aided Design, vol. 44, no. 4, pp. 289-299, 2012.
- [6] F. L. Bookstein, "Principal Warps - Thin-plate Splines and The Decomposition of Deformations," IEEE Transactions on Pattern Analysis and Machine Intelligence, vol. 11, no. 6, pp. 567-585, 1989.